remote sensing

MDPI

Article

A Multi-Cycle Echo Energy Concentration Method for High-Mobility Targets Enveloped by Time-Varying Plasma Sheath

Bowen Bai [1,2], Qingmeng Wang [1,2], Bailiang Pu [1,2,*], Ke Zhang [1,2] and Long Xue [1,2]

[1] Key Laboratory of Equipment Efficiency in Extreme Environment, Ministry of Education, Xidian University, Xi'an 710071, China
[2] School of Aerospace Science and Technology, Xidian University, Xi'an 710071, China
* Correspondence: blp@stu.xidian.edu.cn

Abstract: When a target moves at hypersonic speed, the aerodynamic thermal effect will cause air molecules to form a plasma sheath that envelopes the outer surface of the target, which consists of a large number of charged particles. The plasma sheath imposes a complicated modulation effect on the radar echo signal in terms of amplitude, phase, and frequency. When the plasma sheath is time-varying, the inter-pulse coherence of the multi-cycle echo signals is severely disrupted, resulting in the failure of coherent accumulation. To address the problem of abnormal inter-pulse energy accumulation in targets covered with time-varying plasma sheaths, we analyzed the dynamic modulation effects of time-varying plasma sheaths on echo signals and constructed a radar echo model enveloped with time-varying plasma sheaths. Based on this, we propose a method for inter-pulse energy concentration of multi-cycle echo signals based on range-frequency inversion, second-order Wigner–Ville distribution (WVD), and slow-time symmetric auto-correlation. The proposed method is capable of realizing energy concentration for targets enveloped with time-varying plasma sheaths and can accurately estimate the motion parameters of the target. The effectiveness of our proposed method has been verified via simulation analysis of multi-cycle echo signals from targets enveloped with time-varying plasma sheaths, and the reliability of the method has been further validated through statistical experimental analysis.

Keywords: time-varying plasma sheath; dynamic modulation effect; range-frequency inversion; second-order Wigner–Ville distribution; slow-time symmetric auto-correlation; energy concentration

Citation: Bai, B.; Wang, Q.; Pu, B.; Zhang, K.; Xue, L. A Multi-Cycle Echo Energy Concentration Method for High-Mobility Targets Enveloped by Time-Varying Plasma Sheath. *Remote Sens.* **2024**, *16*, 2316. https://doi.org/10.3390/rs16132316

Academic Editor: Gabriel Vasile

Received: 15 May 2024
Revised: 19 June 2024
Accepted: 20 June 2024
Published: 25 June 2024

1. Introduction

When the speed of a near-space target exceeds Mach 15, the air molecules around the outer surface of the target are dissociated and ionized due to aerothermal ionization, which forms a plasma sheath composed of charged ions, free electrons, and neutral particles enveloping the surface of the target [1]. The plasma sheath imposes a complicated modulation effect on the radar echo signal of the target, which will result in severe waveform distortion in the echo signal and the occurrence of ghost targets in the one-dimensional range profile, severely affecting the reliable radar detection [2–4]. When the above target moves with high maneuverability, its aerodynamic characteristics characterize the plasma sheath with time-varying properties, which are mainly reflected in the time-varying electronic density of the plasma sheath. The time-varying electron density changes the dielectric properties of the plasma sheath, causing radar echo signals to couple with time-varying reflection coefficients. This phenomenon may, further, lead to variations in the initial and final phases of each cycle of the echo signals, resulting in abnormal inter-pulse coherence.

In recent years, with the continuous investigation of near-space targets, achieving reliable detection on near-space targets has become a focus in the field of radar detection. In 2007, Chen et al. found that the plasma sheath modulates the amplitude and phase of radar echoes [5]. Later, they further discovered that the plasma sheath can also reflect

radar signals [6]. It is known that the echo signal consists of many components during the process of radar detection of targets enveloped with plasma sheaths. In 2019, Zhang et al. reproduced the phenomenon of ghost targets on a one-dimensional range profile by simulating the broadband radar signal of targets enveloped with plasma sheaths [7], confirming that the radar echo signals are coupled with multiple Doppler-frequency components. Subsequently, in 2021, Ding et al. revealed the mechanism of "false targets" [8]. Specifically, by constructing a narrowband radar echo model of a plasma-sheath-enveloped target, they analyzed the multi-domain characteristics of radar echo signals under typical heights and speeds. In 2017, based on the measurement data of the RAM-C project, Yao et al. established a spatiotemporal frequency-domain model of targets enveloped with time-varying plasma sheaths and further investigated the statistical characteristics of electromagnetic (EM) wave phase disturbance and amplitude fluctuation caused by time-varying plasma sheaths [9–11]. When the target enveloped with a time-varying plasma sheath exhibits high maneuverability, multi-cycle radar echo signals may also exhibit linear range walk caused by velocity, and second-order range migration and Doppler migration caused by acceleration. In 2005, Zhang et al. effectively accumulated coherence by eliminating the phenomenon of migration through range-cell resolution (MTRC) using the Keystone transformation [12]. Later in 2005, Zhou et al. solved the double-span problem for the target's second-order range migration by adopting the generalized second-order Keystone transformation [13]. Unfortunately, most of the existing energy concentration methods primarily focus on the high speed and high maneuverability of the target, and on the extremely low signal-to-noise ratio (SNR), which fail to eliminate the modulation effect of the time-varying plasma sheath on the echo, causing abnormal accumulation of multi-cycle echo energy.

Currently, the research potential has become significant in the methods for concentrating energy on multi-cycle radar echo signals from targets enveloped with time-varying plasma sheaths. To deal with the problem of abnormal energy accumulation caused by the complex dynamic modulation effect of a time-varying plasma sheath on echo signal, we propose a method utilizing a range-frequency inversion transformation, second-order WVD algorithm, and slow-time symmetric autocorrelation to realize energy concentration of multi-cycle radar echo signals. The feasibility of the proposed method has been verified through simulation experiments, and its detection effect has been evaluated through statistical experimental analysis. It has been verified that our proposed method can effectively concentrate energy and accurately estimate motion parameters while exhibiting high computation efficiency, which is beneficial for theoretical and practical applications.

The key contributions of this study can be summarized as follows: Firstly, by analyzing the impact of the time-varying plasma sheath on echo signals, we formulated a range-frequency inversion, second-order WVD algorithm to minimize the influence of the time-varying plasma sheath. The performance of our proposed method outperformed those of the existing prevailing methods in terms of multi-cycle energy concentration on plasma-sheath-enveloped targets. Secondly, considering the characteristics of high-maneuverability of the target, we adopted the method of acceleration compensation to mitigate the disadvantageous effects caused by the maneuverability of the target. Specifically, we applied symmetric auto-correlation processing to the range-frequency, slow-time signals after acceleration compensation, which not only realizes multi-cycle echo energy concentration of the target enveloped with time-varying plasma sheath but also reduces the computation time of the proposed method. Thirdly, in contrast to existing studies, we constructed a radar echo model for targets enveloped with a time-varying plasma sheath. Based on the method of range-frequency inversion, second-order WVD slow-time symmetric autocorrelation, we achieved energy concentration of multi-cycle radar echo signals for the targets enveloped with a time-varying plasma sheath, compensating for the problem of abnormal energy concentration in multi-cycle radar echo signals caused by the presence of a time-varying plasma sheath. Simulation and experimental analysis

verified the effectiveness of our proposed energy concentration method in the case of the time-varying plasma sheath.

2. Radar Echo Model of Time-Varying, Plasma-Sheath-Enveloped Target

In this study, we take a blunt cone target RAM-C as the model to be analyzed. Due to the non-uniformity of the flow field parameters of the plasma sheath enveloping the target, the target surface can be divided into I reference points, as shown in Figure 1. At each reference point that is perpendicular to the direction of the target surface, the electron density of the plasma sheath approximates a double Gaussian distribution [14], as shown in Figure 2.

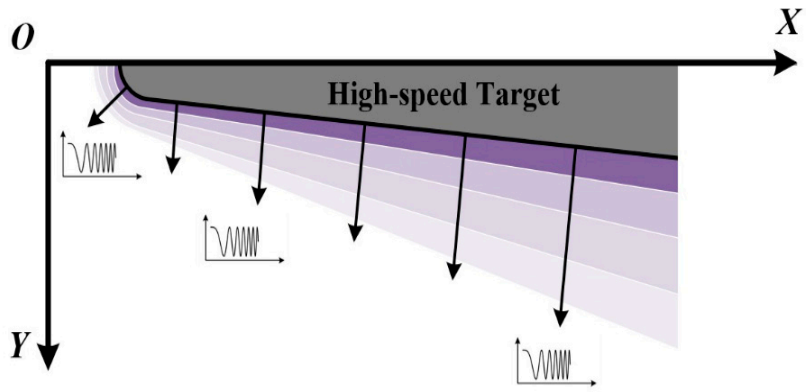

Figure 1. Plasma-sheath-enveloped target model.

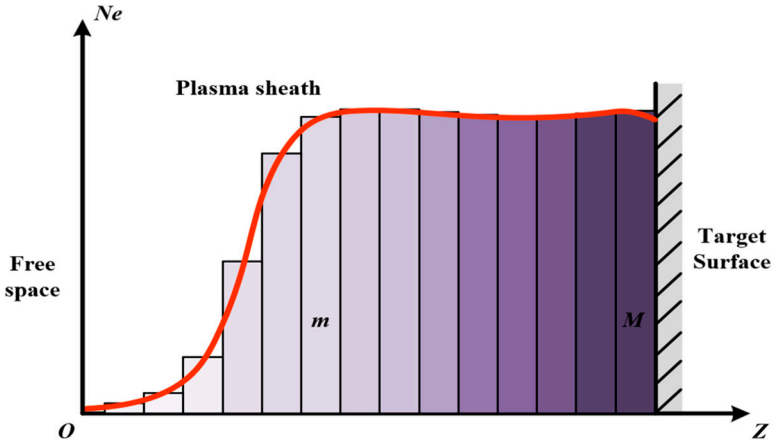

Figure 2. Distribution of electron density on the plasma sheath.

When the target moves with high maneuverability, changes in aerodynamic characteristics cause variations in parameters such as the electron density in the plasma sheath on the target surface, which makes the electron density time-varying. The time-varying electron density further influences the dielectric properties of the plasma sheath. In the case of a time-varying plasma sheath, the radar echo signal will couple with the time-varying characteristics of the electron density, i.e., the radar echo signal will couple with the time-varying maximum reflection coefficient, which, further, causes changes in the initial and final phases of each cycle of the echo signal.

The time-varying electron density model at the i-th reference point can be expressed as

$$Ne_t(i,t) = Ne(i)(1 + r(i,t)) \tag{1}$$

where $Ne(i)$ denotes the electron density distribution at the i-th reference point and $r(i,t)$ denotes the perturbed electron density.

According to the above Equation (1), the time-varying electron density has a steady-state electron density as its initial value, which then oscillates through the perturbed electron density that varies over time. The probability density function (PDF) of the perturbed electron density satisfies

$$P(r(i,t)) = \frac{1}{\sqrt{2\pi}\delta_I} e^{-\frac{[r(i,t)-\mu_I]^2}{2\delta_I{}^2}} \tag{2}$$

where δ_I is the jitter variance of the perturbed electron density and μ_I is the jitter mean of the perturbed electron density.

The power spectral function of the perturbed electron density can be expressed as

$$Ps(r(i,t)) = a_{1,I} e^{-\frac{f^2}{a_{2,I}{}^2}} + b_{1,I} e^{-\frac{(f-f_\delta)^2}{b_{2,I}{}^2}} \tag{3}$$

where f_δ is the central frequency of the perturbed electron density, $a_{1,I}$ is the peak of the first Gaussian power spectrum, $b_{1,I}$ is the peak of the second Gaussian power spectrum, $a_{2,I}$ is the standard deviation of the first Gaussian power spectrum, and $b_{2,I}$ is the standard deviation of the second Gaussian power spectrum.

The time-varying electron density distributed in a local region of the plasma sheath is demonstrated in Figure 3.

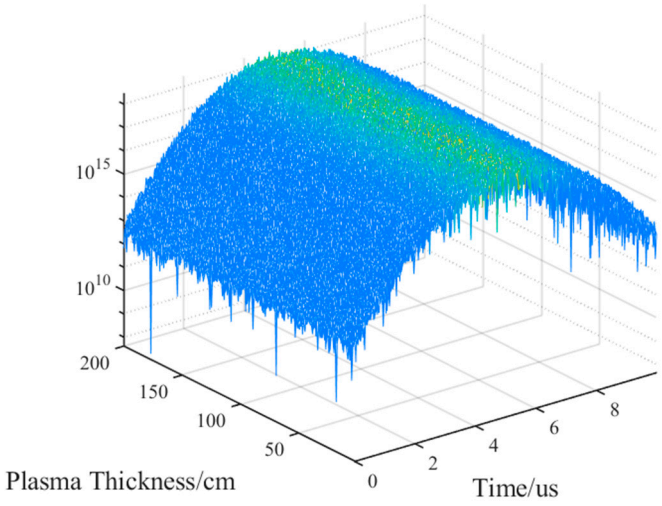

Figure 3. Time-varying electron density distributed in a local region of the plasma sheath.

The plasma sheath at each reference point can be divided into J layers. When EM waves are vertically incident on the target surface, by adopting the method of stratified equivalent wave impedance [15], the time-varying reflection coefficients of the plasma-sheath-enveloped target from the stagnation point to the tail at each layer of each reference point can be calculated by

$$R_{all}(t) = \begin{bmatrix} R_{1,1}(t) & \cdots & R_{1,J}(t) \\ \vdots & R_{i,j}(t) & \vdots \\ R_{I,1}(t) & \cdots & R_{I,J}(t) \end{bmatrix} \tag{4}$$

where $R_{i,j}(t)$ is the time-varying reflection coefficient at layer j of the i-th reference point.

Due to the fact that EM waves have a position of maximum reflection in the time-varying plasma sheath, and that the reflection coefficient at this position has higher energy, the strongest reflection position at each reference point can be described by

$$R_{\max}(t) = \begin{bmatrix} R_1(t) & \cdots & R_I(t) \end{bmatrix} \tag{5}$$

According to the above Equation (5), it is known that the modulation effect of the time-varying reflection coefficient imposed on the echo signal varies dynamically at each instantaneous moment. Therefore, the time-varying reflection coefficient of the multi-period radar echo signal can be expressed as

$$R_{\max}(t) = \begin{bmatrix} R_1(t,m) & \cdots & R_I(t,m) \end{bmatrix} \tag{6}$$

With a linear-frequency-modulated (LFM) signal as the radar's transmission signal, its expression is given by

$$s(t) = rect\left(\frac{t}{T_p}\right)\exp\left(j2\pi\left(f_c + \frac{1}{2}kt^2\right)\right) \tag{7}$$

$$rect\left(\frac{t}{T_p}\right) = \begin{cases} 1, |t| \le T_p/2 \\ 0, |t| > T_p/2 \end{cases} \tag{8}$$

where T_p denotes the pulse width, t denotes the fast time, f_c denotes the carrier frequency, and k denotes the modulation frequency.

The radar echo signal of a target enveloped with the time-varying plasma sheath is the superposition of the echo signals at each reference point on the target enveloped with the time-varying plasma sheath, which can be expressed as

$$s(t,t_m) = \sum_{i=1}^{I} R_i(t,m) rect\left(\frac{t-\tau}{T_p}\right)\exp\left(j2\pi\left((f_c + f_{di})(t-\tau) + \frac{1}{2}k(t-\tau)^2\right)\right) \tag{9}$$

$$rect\left(\frac{t}{T_p}\right) = \begin{cases} 1, |t| \le T_p/2 \\ 0, |t| > T_p/2 \end{cases} \tag{10}$$

In the above Equation (9), $R_i(t,m)$ denotes the maximum reflection coefficient at the i-th reference point (a complex factor affecting the amplitude and phase of the radar echo signal), f_{di} denotes the Doppler frequency coupled at the position corresponding to the maximum reflection coefficient at the i-th reference point, and τ denotes the radar echo delay. Since the detection radar uses a narrowband signal and the target is in the far field, the effect of the interval between the reference points imposed on the target can be neglected. Assuming that the target is always within the same range cell, t_m denotes the slow time, R_0 denotes the initial range between the target and the radar, v_0 denotes the initial velocity of the target, and a denotes the acceleration of the target.

Conducting pulse compression with respect to the radar echo signal, we obtain

$$s_c(t,t_m) = \sum_{i=1}^{I} \begin{array}{l} |R_i(t,m)| Sa\left(\pi B\left(t - \tau + \frac{f_{di}T_p}{B}\right)\right)\exp\left(j2\pi\left(f_c + \frac{f_{di}}{2}\right)t\right) \\ \exp\left(j2\pi\left(f_c + \frac{f_{di}}{2}\right)\tau\right)\exp(j\varphi(R_i(t,m))) \end{array} \tag{11}$$

It can be seen from the above Equation (11) that the function $Sa(\cdot)$ determines the peak position on the one-dimensional range profile of the echo signals, which represents the range between radar and the target. However, due to the presence of the intra-pulse Doppler frequency f_{di}, the peak position will shift accordingly, which will cause the existence of multiple peaks on the one-dimensional range profile. In the case of a time-varying plasma sheath, the pulse compression result of the radar echo is subject to dynamic phase modulation. Due to the dynamics of the plasma sheath, a significant difference exists between its initial and ending phases represented in the range domain of the echo signals amongst different pulses, which may destroy the inter-pulse coherence of the signals.

Coherent accumulation of the range domain characterization results for a target enveloped with a multi-period, time-varying plasma sheath can be calculated by

$$S(l) = \sum_{m=1}^{M} [s_c(t, t_m)] \exp\left(j\frac{2\pi l(m-1)}{M}\right) \tag{12}$$

which can further be expressed as

$$S(l) = \sum_{m=1}^{M} \begin{array}{l} A_0 rect\left(\dfrac{t-\tau^*}{2T_p}\right) \exp(j2\pi(f_0 + f_{di})(t-\tau^*)) SA_1 SA_2 \\ \exp\left(-j\pi\dfrac{M-1}{M}(f_{di}T_r M - l)\right) \exp(j\varphi(R_i(t,m))) \end{array} \tag{13}$$

$$SA_1 = Sa\left(\pi T_p\left(t - \tau^* - \frac{f_{di}}{k}\right)\right) \tag{14}$$

$$SA_2 = Sa(\pi(f_d T_r M - l)) \tag{15}$$

$$\tau^* = \frac{2R_0}{c} \tag{16}$$

where f_d denotes the Doppler frequency corresponding to the target's motion speed.

In the above Equation (13), the function $S(l)$ contains two Sa functions. The intra-pulse Doppler frequency and the inter-pulse Doppler frequency together affect the peak position of the Sa function, and the phase of the time-varying reflection coefficient destroys the inter-pulse coherence of the signal. Therefore, the inter-pulse coherence of the multi-period echo signals from a target enveloped with a time-varying plasma sheath will be affected by ghost targets, high maneuverability characteristics, and the phase of the time-varying reflection coefficient, thereby causing failure of conventional coherent accumulation methods and in the energy concentration.

3. Multi-Cycle Energy Concentration Method for Time-Varying, Plasma-Sheath-Enveloped Target

3.1. Dynamic Modulation Cancellation Technology Based on Frequency-Inversion Second-Order WVD

After conducting pulse compression, the echo signal is subject to fast Fourier transform (FFT) along the fast time axis, resulting in a range-frequency, slow-time signal, which can be expressed by

$$s_c(f_r, t_m) = \sum_{i=1}^{I} \begin{array}{l} A_{i,0} rect\left(\dfrac{f_r - \frac{f_{di}}{2}}{B}\right) \exp(-j2\pi(f_r + f_c)\tau) \exp\left(j2\pi\dfrac{f_{di}T_p}{B} f_r\right) \\ \exp\left(-j\pi\dfrac{{f_{di}}^2 T_p}{B}\right) \exp(j\varphi(R_i(f_r, m))) \end{array} \tag{17}$$

The above Equation (17) can further be written as

$$s_c(f_r, t_m) = \sum_{i=1}^{I} \begin{array}{l} A_{i,0} rect\left(\dfrac{f_r - \frac{f_{di}}{2}}{B}\right) \exp\left(-j2\pi(f_r + f_c)\dfrac{2\left(R_0 + vt_m + \frac{1}{2}a{t_m}^2\right)}{c}\right) \\ \exp\left(j2\pi\dfrac{f_{di}T_p}{B} f_r\right) \exp\left(-j\pi\dfrac{{f_{di}}^2 T_p}{B}\right) \exp(j\varphi(R_i(f_r, m))) \end{array} \tag{18}$$

It can be seen from the above Equation (18) that under the condition of time-varying plasma sheath enveloping, the effect of the plasma sheath imposed on the range-frequency, slow-time signal is reflected in three phase terms, i.e., $\exp(j\varphi(R_i(f_r, m)))$, $\exp\left(j2\pi\frac{f_{di}T_p}{B} f_r\right)$,

and $\exp\left(-j\pi\frac{{f_{di}}^2 T_p}{B}\right)$. Among these, the phase term $\exp(j\varphi(R_i(f_r,m)))$ is the phase of the time-varying reflection coefficient. Between the intra-pulse Doppler frequency and the range frequency, there exists a coupling in the phase term $\exp\left(j2\pi\frac{f_{di}T_p}{B}f_r\right)$. As for the phase term $\exp\left(-j\pi\frac{{f_{di}}^2 T_p}{B}\right)$, it is only correlated with the intra-pulse Doppler frequency of the echo. Since the coupling hinders the accumulation of signal energy, a range-frequency inversion transformation multiplication is performed on the range-frequency, slow-time signal in order to eliminate the influence of the phase term $\exp\left(j2\pi\frac{f_{di}T_p}{B}f_r\right)$ during the signal processing, thereby obtaining

$$\begin{aligned} s_k(f_r,t_m) &= s_c(\overleftarrow{f_r},t_m)\cdot s_c(f_r,t_m) = s_c(-f_r,t_m)\cdot s_c(f_r,t_m) \\ &= \sum_{i=1}^{I} \begin{array}{l} A_{k,0} rect\left(\frac{f_r}{B-f_{di}}\right)\exp\left(-j\frac{8\pi f_c}{c}\left(R_0+v_0t_m+\frac{1}{2}a{t_m}^2\right)\right) \\ \exp\left(j2\pi\frac{{f_{di}}^2 T_p}{B}\right)\exp(j2r(m)) \end{array} + \sum CT_{x,y} \end{aligned} \tag{19}$$

$$\begin{aligned} CT_{x,y} &= M_{x,y}|R_x||R_y| rect\left(\frac{f_r-\frac{f_{dy}-f_{dx}}{4}}{B-\frac{f_{dy}+f_{dx}}{2}}\right)\exp\left(-j\tfrac{8\pi f_c}{c}\left(R_0+v_0t_m+\tfrac{1}{2}a{t_m}^2\right)\right) \\ &\quad\cdot\exp\left(j2\pi\tfrac{(f_{dy}-f_{dx})T_p}{B}f_r\right) \end{aligned} \tag{20}$$

$$M_{x,y} = \exp\left(-j\pi\frac{\left({f_{dx}}^2-{f_{dy}}^2\right)T_p}{B}\right)\exp\left(j\left(\varphi(R_x(f_r,m))-\varphi\left(R_y(f_r,m)\right)\right)\right) \tag{21}$$

In the above Equation (19), the term $s_c(\overleftarrow{f_r},t_m) = s_c(-f_r,t_m)$ denotes the inverse transformation of the signal along the range-frequency axis; $A_{k,0}$ denotes the amplitude, $CT_{x,y}$ denotes the cross term generated during the range-frequency axis inversion multiplication, where x and y satisfy $1 \le x \le I$, $1 \le y \le I$, $x \ne y$; and $M_{x,y}$ is a constant phase term generated during the calculation.

After conducting the range-frequency axis inversion multiplication, the influence of the phase term $\exp\left(j2\pi\frac{f_{di}T_p}{B}f_r\right)$ coupling the range-frequency with the intra-pulse Doppler is eliminated, as well as the coupling between the range frequency f_r and the slow time t_m. In addition, the time-varying nature of the plasma caused by fast-time perturbations in the time-varying reflection coefficient phase term $\exp(j\varphi(R_i(f_r,m)))$ is uncorrelated with the time-varying characteristics of the plasma caused by different signal periods. Therefore, after conducting the range-frequency inversion multiplication, the dimension related to the fast-time frequency is eliminated, whereas the perturbation related to the number of periods is retained, which is denoted as the term $\exp(j2r(m))$. Therefore, by performing inverse fast Fourier transform (IFFT) on the range-frequency dimension of $s_k(f_r,t_m)$, we obtain

$$\begin{aligned} R_k(\hat{t},t_m) &= IFT_{f_r}[s_k(f_r,t_m)] \\ &= \sum_{i=1}^{I} \begin{array}{l} A_{k,1}\sin c\left((B-f_{di})\hat{t}\right)\exp\left(-j\frac{8\pi f_c}{c}\left(R_0+v_0t_m+\frac{1}{2}a{t_m}^2\right)\right) \\ \exp\left(j2\pi\frac{{f_{di}}^2 T_p}{B}\right)\exp(j2r(m)) \end{array} + \sum C_{x,y}^{(1)} \end{aligned} \tag{22}$$

$$\begin{aligned} C_{x,y}^{(1)} &= M_{x,y}A_{k,1}^{(1)}\sin c\left(\left(B-\tfrac{f_{dy}+f_{dx}}{2}\right)\left(\hat{t}+\tfrac{(f_{dy}-f_{dx})T_p}{B}\right)\right) \\ &\quad\cdot\exp\left(j\pi\tfrac{f_{dy}-f_{dx}}{2}\hat{t}\right)\exp\left(-j\tfrac{8\pi f_c}{c}\left(R_0+v_0t_m+\tfrac{1}{2}a{t_m}^2\right)\right) \end{aligned} \tag{23}$$

It can be seen from the above Equation (22) that the signal being performed with IFFT is an Sa function, and the energy of the signal is concentrated at the central position of the $\hat{t} - t_m$ domain. Therefore, by extracting the signal along the slow-time dimension at position $\hat{t} = 0$, we obtain

$$\begin{aligned} R_k(t_m) &= Extract_{t_m}\left[R_k(\hat{t}, t_m)\big|_{\hat{t}=0}\right] \\ &= \sum_{i=1}^{I} A_{k,2} \exp\left(-j\frac{8\pi f_c}{c}\left(R_0 + v_0 t_m + \frac{1}{2}a{t_m}^2\right)\right) \exp\left(j2\pi\frac{{f_{di}}^2 T_p}{B}\right) \exp(j2r(m)) + \sum C_{x,y}^{(2)} \end{aligned} \tag{24}$$

$$C_{x,y}^{(2)} = M_{x,y} A_{k,2}^{(2)} \exp\left(-j\frac{8\pi f_c}{c}\left(R_0 + v_0 t_m + \frac{1}{2}a{t_m}^2\right)\right) \tag{25}$$

where $Extract_{t_m}[\cdot]$ represents the operation of extracting the signal along the slow-time dimension t_m.

After extracting the signal along the slow-time dimension, the two-dimensional signal is transformed into a one-dimensional signal. In subsequent signal processing, the computational complexity is reduced. Because the expression of the signal in the slow-time dimension conforms to the form of a LFM signal, the second-order WVD algorithm can be used to estimate the target's motion acceleration.

The definition of the second-order WVD algorithm is given by

$$R_{SoWVD}(t_m, \tau, \tau_1) = R_k\left(t_m + \frac{\tau}{2}\right) {R_k}^*\left(t_m - \frac{\tau}{2}\right) \cdot \left[R_k\left(t_m + \frac{\tau_1}{2}\right) {R_k}^*\left(t_m - \frac{\tau_1}{2}\right)\right]^* \tag{26}$$

where τ and τ_1 are two time-delay variables. When there is a fixed time-delay difference between τ and τ_1, the coupling among t_m, τ, and τ_1 can be eliminated. Let $\tau_1 = \tau + 2\tau_0$, where τ_0 is a fixed delay.

Further derivations are presented as

$$\begin{aligned} R_{SoWVD}(t_m, \tau; \tau_0) &= R_k\left(t_m + \frac{\tau}{2}\right) {R_k}^*\left(t_m - \frac{\tau}{2}\right) \cdot \left[R_k\left(t_m + \frac{\tau}{2} + \tau_0\right) {R_k}^*\left(t_m - \frac{\tau}{2} - \tau_0\right)\right]^* \\ &= \sum_{i=1}^{I} A_{k,3} \exp\left(j\frac{16\pi f_c}{c}(v_0\tau_0 + a t_m \tau_0)\right) + \sum C_{x,y}^{(3)} \end{aligned} \tag{27}$$

$$C_{x,y}^{(3)} = M_{x,y} A_{k,3}^{(3)} \exp\left(j\frac{16\pi f_c}{c}(v_0\tau_0 + a t_m \tau_0)\right) \tag{28}$$

According to the above Equation (27), the coupling among t_m, τ, and τ_1 has been eliminated by introducing a fixed delay τ_0. In the signal $R_{SoWVD}(t_m, \tau; \tau_0)$, only the variables t_m and τ are included. After conducting the second-order WVD algorithm with respect to $R_k(t_m)$, the effects of the other phase components $\exp(j2r(m))$ and $\exp\left(-j\pi\frac{{f_{di}}^2 T_p}{B}\right)$, that are caused by the time-varying plasma sheath on radar echoes, are removed. Subsequently, performing two-dimensional fast Fourier transform (FFT) on $R_{SoWVD}(t_m, \tau; \tau_0)$, we obtain

$$\begin{aligned} R_{SoWVD}(f_{t_m}, f_\tau) &= FFT_\tau\{FFT_{t_m}[R_{SoWVD}(t_m, \tau; \tau_0)]\} \\ &= A_{k,4} \exp\left(j\tfrac{8\pi f_c}{c} v_0 \tau_0\right) \delta(f_\tau) \delta\left(f_{t_m} - \tfrac{8 f_c a \tau_0}{c}\right) + \sum C_{x,y}^{(4)} \end{aligned} \tag{29}$$

$$C_{x,y}^{(4)} = M_{x,y} A_{k,4}^{(4)} \exp\left(j\frac{8\pi f_c}{c} v_0 \tau_0\right) \delta(f_\tau) \delta\left(f_{t_m} - \frac{8 f_c a \tau_0}{c}\right) \tag{30}$$

It can be seen from the above Equation (29) that after performing two-dimensional FFT, a peak appears in the $f_{t_m} - f_\tau$ domain corresponding to $R_{SoWVD}(f_{t_m}, f_\tau)$, and the peak position $\left(\frac{8 f_c a \tau_0}{c}, 0\right)$ corresponds to the acceleration of the moving target. Therefore, the

acceleration of the target enveloped with the time-varying plasma sheath can be estimated using the peak position, which can be expressed by

$$\hat{a}_k = \frac{c}{8f_c\tau_0}\arg_{f_{t_m}}\max[R_{SoWVD}(f_{t_m}, f_\tau)] \tag{31}$$

3.2. Energy Concentration Method Based on Slow-Time Symmetric Autocorrelation

According to the estimated acceleration, an acceleration compensation function is constructed to eliminate the acceleration exponential terms in the signal, which can be written as

$$H_m(f_r, t_m) = \exp\left(j4\pi(f_r + f_c)\frac{\hat{a}_k {t_m}^2/2}{c}\right) \tag{32}$$

Multiplying the acceleration compensation function with the range-frequency, slow-time signal, we obtain

$$\begin{aligned} Q_k(f_r, t_m) = \sum_{i=1}^{I} & |R_i| rect\left(\frac{f_r - \frac{f_{di}}{2}}{B}\right)\exp\left(-j2\pi(f_r + f_c)\frac{2(R_0 + v_0 t_m)}{c}\right)\exp\left(j2\pi\frac{f_{di}T_p}{B}f_r\right) \\ & \exp\left(-j\pi\frac{{f_{di}}^2 T_p}{B}\right)\exp(j\varphi(R_i(f_r, m))) \end{aligned} \tag{33}$$

The signal model has been transformed from a uniformly accelerated motion model to a uniform motion model. However, since the acceleration compensation function is multiplied by the range-frequency, slow-time signal, the influence of the time-varying plasma sheath on the signal still exists. To eliminate the influence of the plasma sheath on the signal and achieve energy concentration on the multi-period radar echoes, slow-time symmetrical autocorrelation processing is performed on the signal, which is expressed by

$$\begin{aligned} R_m(f_r, \tau_m) &= Q_k(f_r, t_m + \tau_m)Q_k{}^*(f_r, t_m - \tau_m) \\ &= \sum_{i=1}^{I} A_{m,1} rect\left(\frac{f_r - \frac{f_{di}}{2}}{B}\right)\exp\left(-j8\pi\frac{v_0\tau_m}{\lambda}\right)\exp\left(-j8\pi f\frac{v\tau_m}{c}\right)\exp(j2r(m)) + \sum CT^*_{x,y} \end{aligned} \tag{34}$$

$$\begin{aligned} CT^*_{x,y} &= M_{x,y}|R_x||R_y| rect\left(\frac{f - \frac{\min(f_{dx}, f_{dy}) + \max(f_{dx}, f_{dy})}{4}}{B + \frac{\min(f_{dx}, f_{dy}) - \max(f_{dx}, f_{dy})}{4}}\right)\exp\left(-j8\pi f_r\frac{v_0\tau_m}{\lambda}\right) \\ &\quad \cdot \exp\left(-j8\pi f_r\tau_m\left(\frac{v}{c} - \frac{(f_{dx} - f_{dy})T_p}{4B\tau_m}\right)\right) \end{aligned} \tag{35}$$

In the above Equation (34), $A_{m,1}$ denotes the amplitude, τ_m denotes the time delay (usually an integer multiple of the pulse repetition period), and $CT^*_{x,y}$ denotes the cross-term generated after performing slow-time symmetrical autocorrelation. After conducting slow-time symmetrical autocorrelation with respect to $Q_k(f_r, t_m)$, the phase effects caused by the plasma sheath on the signal are effectively removed. In addition, because the acceleration exponential term is eliminated, the term $R_m(f_r, \tau_m)$ is independent of t_m. Due to the coupling that exists between f_r and τ_m, variable scale inverse Fourier transform (SCIFT) is performed to realize decoupling. Performing SCIFT and FFT with respect to $R_m(f_r, \tau_m)$, we obtain

$$\begin{aligned} C_m(\hat{t}_{\tau_m}, f_{\tau_m}) &= FFT_{\tau_m}\left\{SIF_{f_r}[R_m(f_r, \tau_m)]\right\} \\ &= \sum_{i=1}^{I} A_{m,2}\sin c\left(B\left(\hat{t}_{\tau_m} - \frac{4v}{\beta c}\right)\right)\exp\left(j\pi f_{di}\left(\hat{t}_{\tau_m} - \frac{4v}{\beta c}\right)\right)\delta\left(f_{\tau_m} + \frac{4v_0 f_0}{c}\right) \end{aligned} \tag{36}$$

where $\hat{t}_{\tau_m}$ denotes the equivalent fast time after SCIFT, and f_{τ_m} denotes the frequency after FFT.

According to the above Equation (24), after performing SCIFT and FFT, the signal energy accumulates peaks in the $\hat{t}_{\tau_m} - f_{\tau_m}$ plane. Based upon the position of these peaks, the target's velocity can be estimated as

$$v_k = \frac{\beta c}{4} \arg_{\hat{t}_{\tau_m} - f_{\tau_m}} \max \left[C_m \left(\hat{t}_{\tau_m}, f_{\tau_m} \right) \right] \tag{37}$$

where β is the scale transformation factor that is mainly used to adjust the parameter range.

This study proposes a multi-cycle energy concentration method for targets enveloped with a time-varying plasma sheath based on range-frequency inversion, second-order WVD slow-time symmetric autocorrelation. Specifically, the proposed algorithm utilizes range-frequency inversion multiplication combined with second-order WVD processing to eliminate the dynamic modulation effects of the time-varying plasma sheath on echo signals, and to estimate the acceleration of moving targets. Then the acceleration-compensated signals are processed by slow-time symmetric autocorrelation to concentrate the energy of multi-cycle radar echoes, thereby estimating the target's motion speed. The flow of the proposed method is demonstrated in Figure 4.

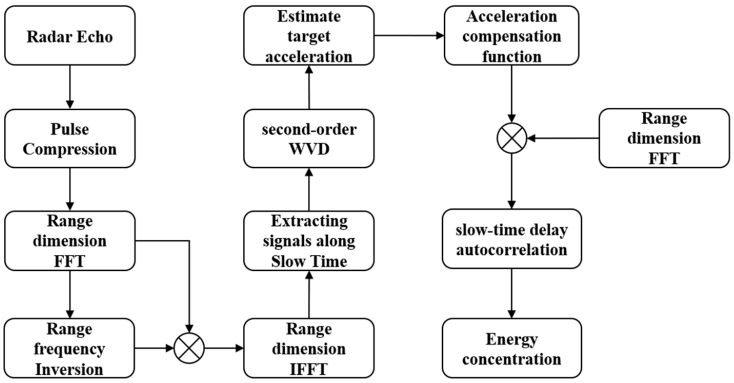

Figure 4. Flowchart of the proposed method.

4. Simulation Verification

This section verifies the impact of the time-varying plasma sheath imposed on radar echo signals, which includes the coupling of multiple intra-pulse Doppler frequencies and the abnormal inter-pulse coherence of multi-cycle radar echoes. Additionally, the proposed method has been analyzed and validated via simulation, demonstrating its reliability and effectiveness.

In Table 1, the simulation parameters are set based on typical radar detection parameters of plasma-sheath-enveloped targets.

Table 1. Parameter setting of the simulation.

Parameter Setting	Values
Initial range	R = 30 km
Carrier frequency	f_c = 5.8 GHz
Pulse width	T_p = 100 μs
Bandwidth	B = 10 MHz
Sampling frequency	F_s = 20 MHz
Pulse repetition interval	T_r = 220 μs
Number of pulses	M = 512
Velocity	v_0 = 6800 m/s
Acceleration	a = 200 m/s^2

4.1. Echo Signal Processing for Target Enveloped with Time-Varying Plasma Sheath

The simulation involves pulse compression and coherent accumulation of multi-cycle radar echo signals from a target enveloped with a time-varying plasma sheath, for which the results are depicted in Figure 5.

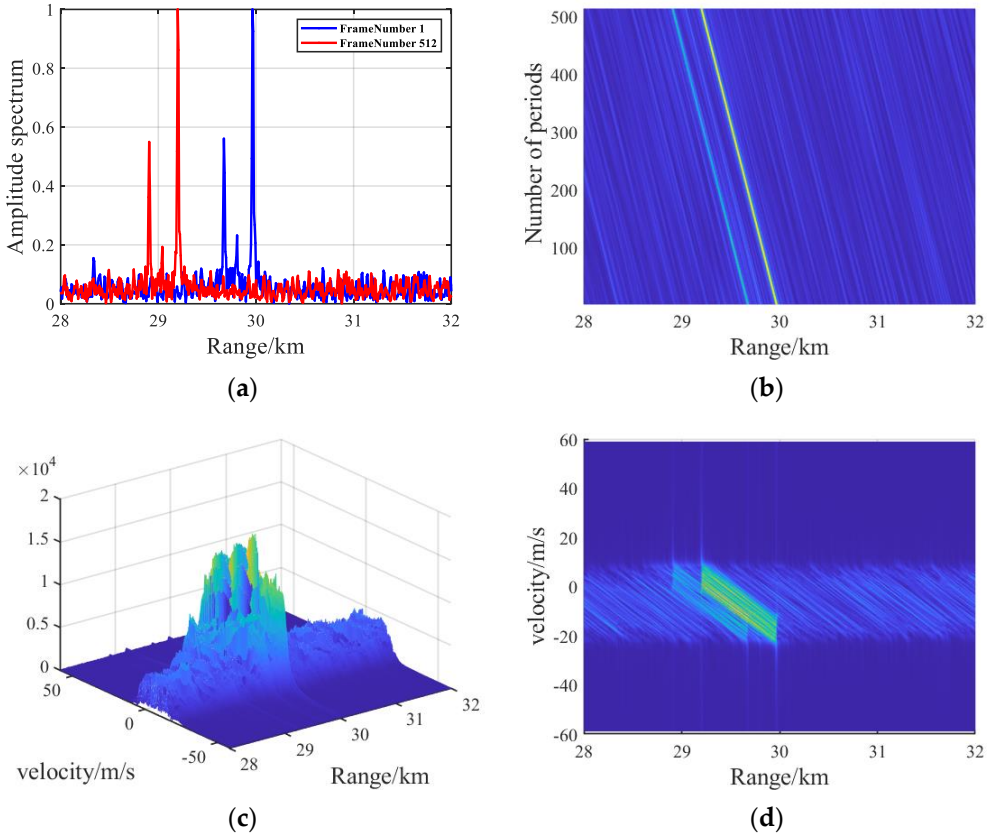

Figure 5. Pulse compression results of (**a**) the first and last cycles of target enveloped with time–varying plasma sheath and (**b**) multi–cycle echo signals. (**c**) Coherent accumulation results of the target enveloped with time–varying plasma sheath. (**d**) Energy diagram of coherent accumulation results for the target enveloped with time–varying plasma sheath.

It can be observed from Figure 5a that due to the gradual decrease in peak electron density at each reference point from the area of the stationary point to that of the tail end, the incident depth of EM waves varies at different reference points on the target surface, and the coupled Doppler-frequency changes, which causes the occurrence of ghost targets in one-dimensional range profile (i.e., multiple peaks occur in the one-dimensional range profile). The pulse compression results from the first and the 512th cycle echoes suggest that due to the high speed of the target enveloped with the time-varying plasma sheath, their movement exceeds the radar's range-cell resolution, causing a significant shift in the peaks.

It can be observed from Figure 5b that when the plasma-sheath-enveloped target exhibits high maneuverability, multi-cycle radar echo signals undergo both range-cell migration and Doppler shift, resulting in multiple slant lines on the two-dimensional period-range plane. Furthermore, due to the time-varying characteristics of the plasma sheath, the time-varying coefficient dynamically disturbs the amplitude and phase of the echo signals, causing a certain degree of diffusion phenomenon in the energy distribution of the two-dimensional periodic range plane.

Figure 5c,d suggest that when the plasma sheath is time-varying, the inter-pulse coherence of multi-cycle radar echo signals is disrupted. After performing pulse compression, the echo signals are processed with coherent accumulation. Due to the effects of range walk,

Doppler shift, ghost targets, and time-varying reflection coefficients, the peak energy of the coherent accumulation undergoes severe dispersion, making it impossible to estimate the target's motion speed by peak energy.

The simulation results for performing conventional coherent accumulation methods to concentrate the energy of multi-cycle echo signals from the target enveloped with time-varying plasma sheath are demonstrated in Figure 6.

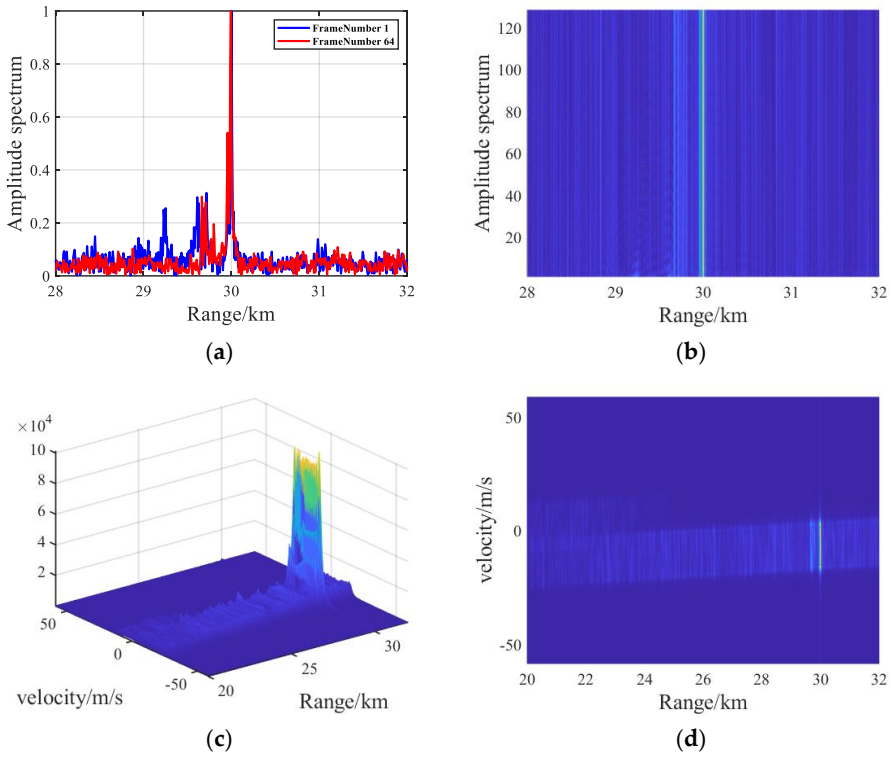

Figure 6. Pulse compression results of (**a**) the first and last cycles of the target enveloped with time–varying plasma sheath after correction and (**b**) multi–cycle echo signals after correction. (**c**) Coherent accumulation results of the target enveloped with time-varying plasma sheath after correction. (**d**) Energy diagram of coherent accumulation results of the target enveloped with time–varying plasma sheath after correction.

It can be observed from Figure 6a,b that adopting conventional compensation methods can eliminate the range walk and Doppler shift caused by the high maneuverability of the target enveloped with a time-varying plasma sheath. Unfortunately, these methods fail to eliminate the dynamic modulation effects caused by the time-varying plasma sheath on the radar echoes, resulting in multiple significant straight lines and ongoing dispersion on the two-dimensional period-range plane.

Figure 6c,d reveal that the time-varying nature of the plasma sheath causes changes in the initial and final phases of each cycle's echo signals. When processing the compensated echo signals with coherent accumulation, the disruption of inter-pulse coherence causes energy leakage in the peak values after coherent accumulation. The problem of energy dispersion caused by the time-varying characteristics of the plasma sheath remains unresolved.

4.2. Simulation Verification

The problem of abnormal coherent accumulation of multi-cycle echo signals from the target enveloped with time-varying plasma sheaths is mainly caused by anomalies in pulse-to-pulse coherence due to changes in the phase of the time-varying reflection coefficient. In response to the above problem, this study considers a noise-free, single-target experimental scenario. Specifically, we analyzed the feasibility of the proposed method in accumulating energy from multi-cycle echo signals under various degrees of simulated random phase

disturbances while maintaining the same flight altitude, speed, and acceleration conditions. And to verify the feasibility of the proposed method in practical applications, the noise resistance of the proposed method was analyzed.

It can be observed from Figure 7 that in the absence of random phase disturbances, although the echo signals among each cycle are coherent, multiple intra-pulse Doppler frequencies are still coupled within the echoes. The method proposed in this study is capable of eliminating the coupled intra-pulse Doppler frequencies within the echo signals, concentrating the energy of the multi-cycle echo signals while realizing the estimation of the target's motion speed. The estimated value of the target's motion acceleration is $a = 200.03\ \mathrm{m/s^2}$ with an estimation error of $\Delta a = 0.03\ \mathrm{m/s^2}$, which is less than the order of magnitude of 10^{-1}. The estimated value of the target's motion speed is $v = 6796\ \mathrm{m/s}$, with a speed estimation error of $\Delta v = 4\ \mathrm{m/s}$, and the error is within 1 order of magnitude.

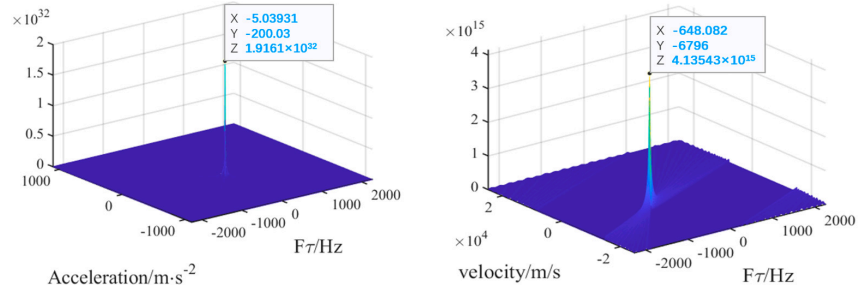

(**a**) (**b**)

Figure 7. (**a**) Estimation results of acceleration without random phase. (**b**) Energy concentrating results without random phase disturbances.

It can be observed from Figure 8 that when the plasma sheath exhibits time-varying characteristics, the proposed method effectively minimizes the dynamic modulation effects caused by the time-varying plasma sheath on echo signals. This is realized through range-frequency inversion multiplication and second-order WVD on the range-frequency, slow-time signals. These techniques not only mitigate the dynamic modulation effects but also eliminate the range walk and Doppler migration phenomena associated with high-maneuvering target. As a result, the energy peaks become significantly prominent in the domain of $f_{t_m} - f_\tau$, enabling accurate estimation of the target's motion acceleration at $a = 200.03\ \mathrm{m/s^2}$ with an estimation error of $\Delta a = 0.03\ \mathrm{m/s^2}$, where the error is less than the order of magnitude of 10^{-1}. After compensating for the acceleration affected by the time-varying plasma sheath and applying slow-time symmetric autocorrelation to the signals, the method concentrates the energy of multi-cycle echo signals. From the location of the peak values, the estimated target motion speed is $v = 6796\ \mathrm{m/s}$ with a speed estimation error of $\Delta v = 4\ \mathrm{m/s}$, and the error remains within 1 order of magnitude.

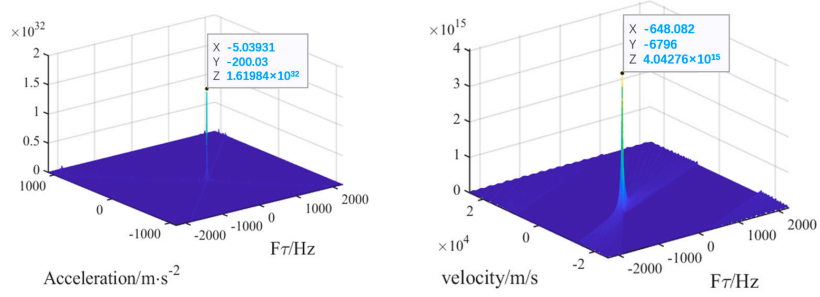

(**a**) (**b**)

Figure 8. *Cont.*

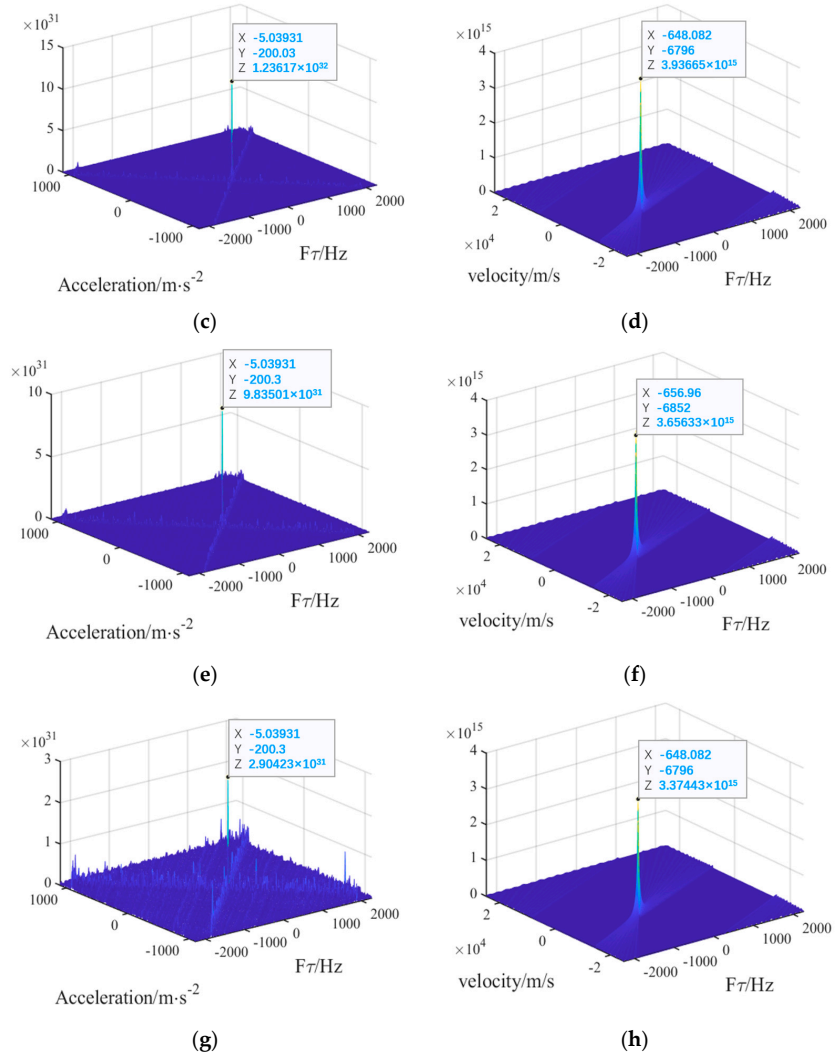

Figure 8. (**a**) Estimation results for acceleration with random phase disturbances ranging from 0 to 30°. (**b**) Energy concentration results with random phase disturbances from 0 to 30°. (**c**) Acceleration estimation results with random phase disturbances ranging from 0 to 45°. (**d**) Energy concentration results when random phase disturbances are 0–45°. (**e**) Acceleration estimation results with random phase disturbances ranging from 0 to 60°. (**f**) Energy concentration results when random phase dis–turbances are 0–60°. (**g**) Acceleration estimation results with random phase disturbances ranging from 0 to 90°. (**h**) Energy concentration results when random phase disturbances are 0–90°.

The noise resistance performance of the proposed method is shown in Figure 9.

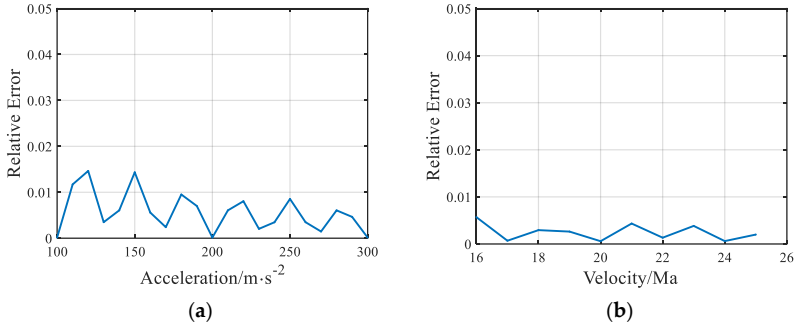

Figure 9. Relative error curve of the estimation of (**a**) target motion acceleration and (**b**) target motion speed.

It can be observed from Figure 10 that when the time-varying plasma sheath imposes complex dynamic modulation effects on the radar echo in terms of amplitude, phase, and frequency, the proposed method can concentrate the energy of multi-cycle echo signals from targets enveloped with the time-varying plasma sheath at SNR > −16 dB. When the SNR is greater than −16 dB, the proposed method can accurately estimate the motion parameters of the target, suggesting that the algorithm still exhibits good performance in low SNR situations (i.e., strong noise resistance).

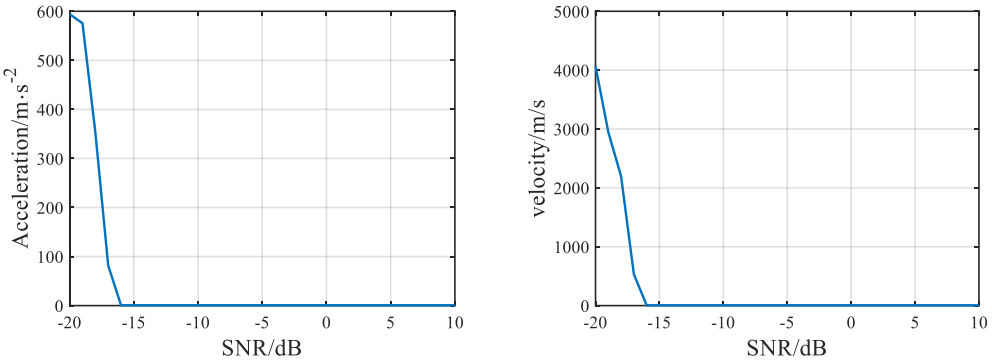

(**a**) (**b**)

Figure 10. Error curves of the estimation of (**a**) target motion acceleration and (**b**) target motion speed.

It can be observed from Figure 9 that when the target's moving speed varies, the relative error of speed estimation is less than 1%. When the acceleration of the target varies, the relative error of the acceleration estimation is less than 2%. As target motion parameters vary, the relative error remains in a small error range, which proves that the proposed method has certain universality.

5. Conclusions

This study analyzes the complex dynamic modulation effects of time-varying plasma sheath imposed on radar echo signals. By simulating the radar echo model of the target enveloped with the time-varying plasma sheath, it has been verified that the plasma sheath can cause the occurrence of ghost targets in single-cycle radar echo signals and abnormalities in inter-pulse coherence and energy accumulation in multi-cycle echo signals. To solve the problem of abnormal multi-cycle echo signal energy concentration caused by the time-varying plasma sheath, we proposed a method based on range-frequency inversion, second-order WVD, and slow-time symmetric autocorrelation. Our proposal effectively mitigates the dynamic modulation effects induced by the time-varying plasma sheath through range-frequency inversion multiplication and second-order WVD, thereby enabling accurate acceleration estimation of the plasma-sheath-enveloped target. Following acceleration compensation of the signals, we performed slow-time symmetric autocorrelation processing on the echo signals to concentrate the energy of the multi-cycle echo signals and to estimate the motion velocity of the target. The simulation results have proved the effectiveness of the proposed method in suppressing the dynamic modulation effects caused by the time-varying plasma sheath, concentrating the energy of multi-cycle echo signals, while maintaining excellent performance even at low SNRs. According to the peak position of energy accumulation, the accurate estimation of the motion parameters of time-varying, plasma-sheath-enveloped target can be obtained. And the relative error of motion parameter estimation is kept in a small range, proving that the proposed method possesses excellent applicability for targets with different motion parameters. This provides a valuable approach for the study of energy concentration in multi-cycle radar echo signals from targets enveloped with time-varying plasma sheath.

Despite the aforementioned research findings, only the anomalous inter-pulse coherence caused by time-varying reflection coefficients on multi-cycle echo signals was

considered in the experimental setup, whereas the random disturbance generated by time-varying reflection coefficients on the instantaneous time of echo signals was neglected. This defect may affect the practical application of our proposed method. Our future research interests will focus on more refined modeling of target radar echoes enveloped with time-varying plasma sheaths, thereby eliminating the impact of time-varying plasma sheaths on echo signals while laying theoretical foundation for improving the generality and robustness of multi-cycle echo signal energy concentration.

Author Contributions: Conceptualization, B.B. and Q.W.; methodology, B.B.; formal analysis, B.B., Q.W., B.P., K.Z. and L.X.; investigation, B.B., Q.W. and B.P.; writing—original draft preparation, Q.W.; writing—review and editing, B.B.; supervision, B.B. All authors have read and agreed to the published version of the manuscript.

Funding: This work was supported partially by the National Natural Science Foundation of China under Grant Nos. 62171349, 92371205, and 62001388, and partially by the Natural Science Basic Research Plan in Shaanxi Province of China under Grant No. 2020JM-102.

Data Availability Statement: The original contributions presented in the study are included in the article, further inquiries can be directed to the corresponding author.

Acknowledgments: The authors would like to thank the handling editor and the anonymous reviewers for their careful reading and helpful remarks.

Conflicts of Interest: The authors declare no conflicts of interest.

References

1. Hartunian, R.A.; Stewart, G.E.; Fergason, S.D.; Curtiss, T.J.; Seibold, R.W. *Causes and Mitigation of Radio Frequency (RF) Blackout during Reentry of Reusable Launch Vehicles*; No. ATR-2007 (5309)-1; Aerospace Corporation: El Segundo, CA, USA, 2007.
2. Dix, D.M. *Typical Values of Plasma Parameters Around a Conical Re-Entry Vehicle*; Scientific Report AD295429; Aerospace Corporation: El Segundo, CA, USA, 1962.
3. Close, S.; Oppenheim, M.; Hunt, S.; Dyrud, L. Scattering characteristics of high-resolution meteor head echoes detected at multiple frequencies. *J. Geophys. Res. Space Phys.* **2002**, *107*, SIA 9-1–SIA 9-12. [CrossRef]
4. Liu, S.H.; Guo, L.X. Analyzing the electromagnetic scattering characteristics for 3-D inhomogeneous plasma sheath based on PO method. *IEEE Trans. Plasma Sci.* **2016**, *44*, 2838–2843. [CrossRef]
5. Kero, J.; Szasz, C.; Wannberg, G.; Pellinen-Wannberg, A.; Westman, A. On the meteoric head echo radar cross section angular dependence. *Geophys. Res. Lett.* **2008**, *35*, 154–162. [CrossRef]
6. Chen, X.-Y.; Li, K.-X.; Zhou, Y.-G.; Li, X.-P.; Liu, Y.-M. Study of the influence of time-varying plasma sheath on radar echo signal. *IEEE Trans. Plasma Sci.* **2017**, *45*, 3166–3176. [CrossRef]
7. Zhang, X.; Liu, Y.; Bai, B.; Li, X.; Shen, F.; Chen, X.Y.; Zhao, L. Establishment of a wideband radar scattering center model of a plasma sheath. *IEEE Access* **2019**, *7*, 140402–140410. [CrossRef]
8. Ding, Y.; Bai, B.; Gao, H.; Niu, G.; Shen, F.; Liu, Y.; Li, X. An analysis of radar detection on a plasma sheath covered reentry target. *IEEE Trans. Aerosp. Electron. Syst.* **2021**, *57*, 4255–4268. [CrossRef]
9. Shi, L.; Liu, Y.; Fang, S.; Li, X.; Yao, B.; Zhao, L.; Yang, M. Adaptive multistate Markov channel modeling method for reentry dynamic plasma sheaths. *IEEE Trans. Plasma Sci.* **2016**, *44*, 1083–1093. [CrossRef]
10. Yao, B.; Li, X.; Shi, L.; Liu, Y.; Zhu, C. A multiscale model of reentry plasma sheath and its nonstationary effects on electromagnetic wave propagation. *IEEE Trans. Plasma Sci.* **2017**, *45*, 2227–2234. [CrossRef]
11. Yao, B.; Li, X.; Shi, L.; Liu, Y.; Lei, F.; Zhu, C. Plasma sheath: An equivalent nonlinear mirror between electron density and transmitted electromagnetic signal. *Phys. Plasmas* **2017**, *24*, 102104. [CrossRef]
12. Zhang, S.S.; Zeng, T. Weak target detection based on keystone transform. *Dianzi Xuebao (Acta Electron. Sin.)* **2005**, *33*, 1675–1678.
13. Zhou, F.; Wu, R.; Xing, M.; Bao, Z. Approach for single channel SAR ground moving target imaging and motion parameter estimation. *IET Radar Sonar Navig.* **2007**, *1*, 59–66. [CrossRef]
14. Rawhouser, R. Overview of the AF avionics laboratory reentry electromagnetics program. *NASA Spec. Publ.* **1971**, *252*, 3.
15. Ding, Y.; Bai, B.; Gao, H.; Liu, Y.; Li, X.; Zhao, M. Method of detecting a target enveloped by a plasma sheath based on Doppler frequency compensation. *IEEE Trans. Plasma Sci.* **2020**, *48*, 4103–4111. [CrossRef]